

STIC-ILL

mpl

From: Holleran, Anne
Sent: Monday, May 10, 2004 12:36 PM
To: STIC-ILL
Subject: refs. for 09/743,684

Please send copies of the following papers:

1. Stevens Biochemistry (1993) 32: 4051-4059
2. Fluharty Biochem. Med. Metab. Biol. (1992) 47: 66-85
3. Faull J. Mass Spectrom (2000) 35: 1416-1424
4. Faull J. Mass Spectrom (1999) 34: 1040-1054

Anne Holleran
AU: 1642
Tel: (571) 272-0833
RM: Remsen, 3A14

mailbox: Remsen, 3C18

32: 4051-4059
Biochem. Med. Metab. Biol.
35: 1416-1424
1040-1054

32: 4051-4059
Biochem. Med. Metab. Biol.
35: 1416-1424
1040-1054

Cerebroside Sulfate Activator Protein (Saposin B): Chromatographic and Electrospray Mass Spectrometric Properties

Kym F. Faull,^{1*} Julian P. Whitelegge,¹ Jason Higginson,¹ Trang To,² Jeffrey Johnson,² Andrew N. Krutchinsky,³ Kenneth G. Standing,³ Alan J. Waring,⁴ Richard L. Stevens,¹ Claire B. Fluharty² and Arvan L. Fluharty²

¹ Pasarow Mass Spectrometry Laboratory, Department of Psychiatry and Biobehavioral Sciences and the Neuropsychiatric Institute and Department of Chemistry and Biochemistry, UCLA, Los Angeles, California 90095, USA

² Mental Retardation Research Center, Department of Psychiatry and Biobehavioral Sciences and the Neuropsychiatric Institute, University of California, Los Angeles, California 90024, USA

³ Physics Department, University of Manitoba, Winnipeg, Manitoba R3T2N2, Canada

⁴ Departments of Pediatrics, Drew University–King Medical Center/UCLA, Los Angeles California 90059, USA

Cerebroside sulfate activator protein is a small, heat-stable protein that is exceptionally resistant to proteolytic attack. This protein is essential for the catabolism of cerebroside sulfate and several other glycosphingolipids. Protein purified from pig kidney and human urine was extensively characterized by reversed-phase liquid chromatography and electrospray mass spectrometry. These two sources revealed 20 and 18 different molecular isoforms of the protein, respectively. Plausible explanations of the structures of the majority of these isoforms can be made on the basis of accurate molecular mass assignments. The reversed-phase chromatographic and electrospray mass spectrometric properties of enzymatically deglycosylated and disulfide-reduced protein were also compared. In addition to a demonstration of the power of electrospray ionization mass spectrometry for revealing a wealth of information on protein microheterogeneity and structural detail, the results also demonstrate the utility of this technique for monitoring spontaneous chemical and enzymatically mediated changes that occur as a result of metabolic processing and protein purification. Copyright © 1999 John Wiley & Sons, Ltd.

KEYWORDS: pig kidney and human urine cerebroside sulfate activator protein; saposin B; electrospray mass spectrometry; reversed-phase high-performance liquid chromatography

INTRODUCTION

Because lipid binding and transport proteins facilitate lipid transport in an aqueous environment, they are essential for normal cellular function. There are two main classes of lipid binding proteins: the so-called β -sheet clam structures¹ and the α -helical amphipathic barrel structures.² Cerebroside sulfate activator (CSAct), which belongs to the second of these classes, and related proteins have been collectively referred to as saposin-like proteins in recognition of a common structural motif³ consisting of 4–5 helical bundles with 45–60% α -helical content and conserved sequence homology which includes three disulfide bridges, a set of hydrophobic residues and a glycosylation site. This class of proteins, which is widely distributed in nature, has also been referred to as swaposins

in recognition of circular permutations within the encoding genes.⁴ NMR investigations of another member of this protein class (NK-lysin) have suggested the presence of a common fold in their solution conformation.⁵ As a class they have not yet been extensively studied and their structures and modes of action are poorly understood. CSAct is the best known example of this class of proteins and represents a model system for their study.

CSAct, a small, heat-stable protein which is exceptionally resistant to proteolytic enzymes, is involved in the catabolism of cerebroside sulfate (CS) and several other glycosphingolipids^{6,7} (for reviews see Refs. 8–12). It has been referred to by a number of names including sphingolipid activator protein 1 (SAP-1),¹³ saposin B⁹ and the non-specific activator protein.¹⁴ Genetic defects in human CSAct lead to arylsulfatase A-positive forms of metachromatic leukodystrophy,^{15,16} a progressive neurodegenerative disease.¹⁷ The gene for the precursor to CSAct, prosaposin, has been cloned^{18–21} and several disease-related mutations identified (see Ref. 10 for summary). One function of CSAct involves extraction of a lipid ligand from membrane fragments incorporated into lysosomes and presentation of the lipid substrate to arylsulfatase A or other enzymes for hydrolysis of the sulfate group or other hydrophobic adducts.¹¹ However, it is

*Correspondence to: K. F. Faull, Department of Chemistry and Biochemistry, UCLA, 405 Hilgard Avenue, Los Angeles, California 90095, USA.

E-mail: faull@chem.ucla.edu

Contract/grant sponsor: NIH; Contract/grant number: NS31271, PI. ALF.

Contract/grant sponsor: W. M. Keck Foundation.

Contract/grant sponsor: NSERC (Canada).

thought that this protein also facilitates the transport of lipids between membranes,^{22,23} and the incomplete overlapping tissue distributions of CSAct and CS suggests the possibility of yet additional unknown functions.

A full description of the three-dimensional coordinates of the protein, delineation of the hydrophobic and hydrophilic surfaces and knowledge of the folding of the polypeptide chain will be necessary before a complete understanding of the mechanism of lipid sequestration and release is possible. These features must explain the paradoxical properties of aqueous solubility with the simultaneous ability to bind lipid ligands, exceptional heat stability and resistance to proteolytic enzymes. Pig kidney²⁴ and human urine²⁵ are rich sources of CSAct from which milligram quantities of highly purified protein can be obtained. We present here details of the chromatographic and electrospray (ESI) mass spectrometric behavior of CSAct from these two sources.

EXPERIMENTAL

Materials

Trifluoroacetic acid (TFA) (HPLC grade in 1 ml glass ampoules) was purchased from Pierce (Rockford IL, USA), acetonitrile (HPLC grade) and methanol (Optima grade) from Fischer Scientific (Tustin, CA, USA), *N*-glycosidase F (PNGase F) and *N*-glycosidase A from Boehringer Mannheim (Mannheim, Germany), dithiothreitol (DTT) from Gibco BRL Life Technologies, New York, USA, dialysis membranes (Spectra/Por 3) from Spectrum Medical Industries (Los Angeles, CA, USA) and bovine brain cerebroside sulfate (CS) and synthetic palmitoyl sulfatide from Matreya (Pleasant Gap, PA, USA). [³⁵S]CS was purified from rat brain as previously described.²⁶ Quartz-distilled ultrapure water (>16 mOhm cm⁻¹) was produced in-house and all other reagents and solvents were of analytical grade or better.

CSAct purification

Pig kidney activator (PKA) was prepared from kidneys as previously described,²⁴ with minor modifications, by sequential lectin affinity (Con A Sepharose, eluted with methyl α -D-mannopyranoside), hydrophobic interaction (octyl Sepharose CL-4B, eluted with octyl α -D-glucopyranoside), anion exchange (QMA, eluted with a sodium chloride gradient) and finally size exclusion (Sephacryl S-300 HF, eluted with 25 mM Tris-HCl, pH 7.5) chromatography. The final eluate was concentrated in a pressurized filtration apparatus (Amicon Diaflo Ultrafilter, YM2 membrane, 3 kDa molecular mass cut-off, under 40 psig nitrogen pressure) to about 27 mg ml⁻¹ protein (Lowry protein assay using bovine serum albumin (BSA) as standard). This preparation is henceforth referred to as native PKA.

Human urine activator (HUA) was prepared from pooled urine as previously described²⁵ using ammonium sulfate (80% saturation) precipitation of urinary proteins and the same series of sequential chromatography as described for PKA. The fraction used in these experiments

was that which was not retained by Con A Sepharose. The final eluate was concentrated as described for PKA to between 3 and 7.5 mg ml⁻¹ protein. This preparation is henceforth referred to as native HUA.

Enzymatic deglycosylation of CSAct

Native PKA (27 mg ml⁻¹ protein, 1.25 ml aliquots) and HUA (3 mg ml⁻¹ protein, 2 ml aliquots) were diluted with sodium phosphate buffer (100 mM, pH 7.0, containing 25 mM EDTA; 1 ml buffer/CSAct aliquot) to which was added *N*-glycosidase F (40 units for PKA, 20 units for HUA in 100 mM sodium phosphate, 25 mM EDTA, 5 mM sodium azide and glycerol, 50% (v/v), pH 7.2, 2 units/ μ l). The reaction mixtures were kept under a slight positive pressure of argon to minimize the opportunity for protein oxidation and incubated at 37°C. To monitor the progress of the reaction, aliquots (1 μ l) were diluted in water-acetonitrile-formic acid (50:50:0.1, v/v/v; 100 μ l) and analyzed by flow injection ESI. During the incubation there was a progressive disappearance of the signals for the pentasaccharide-containing glycoforms (5-CHO) and the appearance of signals corresponding to deglycosylated protein (0CHO), with virtually no change in the intensity of the signals for the disaccharide and monosaccharide-containing glycoforms (2CHO and 1CHO, respectively) (2CHO, 1CHO, etc. represent two, one, etc. sugar adduct). When the concentration of the 0CHO glycoform maximized (typically after 4–7 days of incubation) the mixture was frozen and the components were subsequently separated by C₈ reversed-phase high-performance liquid chromatography (RP-HPLC). Similar results were obtained with *N*-glycosidase F isolated from culture filtrates of *Flavobacterium meningosepticum* and with cloned enzyme isolated from culture filtrates of *E. coli* which had been engineered to express the enzyme. *N*-Glycosidase A from almonds was ineffective at hydrolyzing the carbohydrate moiety from native PKA.

Preparation of reduced protein

Dried native PKA and HUA were treated with guanidine HCl (6 M) containing sodium phosphate buffer (100 mM, pH 7.3) and DTT (1 M) at room temperature for 1 h. Reaction mixtures typically had between 0.4 and 12 mg of protein dissolved in 300–1000 μ l. The reaction mixture was then desalted by C₄ RP-HPLC. Fractions containing the reduced protein were pooled, dried in a vacuum centrifuge, redissolved in an appropriate solvent and the protein was estimated from the OD₂₈₀ reading (optical density at 280 nm). The state of disulfide reduction was judged from the measured molecular mass of the protein determined from the ESI spectra of samples diluted to about 20 pmol μ l⁻¹ in water-acetonitrile-formic acid (50:50:0.1), and following reaction with 4-vinylpyridine. The reduced protein was 6 Da heavier than the non-reduced protein and showed a mass increase of 630 Da following reaction with 4-vinylpyridine (105.1 Da mass increase expected for incorporation of each pyridoethyl group; data not shown).

Reversed-phase HPLC

Isoforms of native CSAct and components of deglycosylation reaction mixtures were purified by C₈ RP-HPLC using the gradient system previously described.²⁷ Column loadings of up to 27 mg of protein per run were tolerated without compromising the separation of deglycosylated from residual glycosylated isoforms on semi-preparative columns (Keystone Scientific Betasil C₈, 250 × 10 mm i.d., 5 µm particle size, 100 Å pore size) at a flow-rate of 3 ml min⁻¹. Smaller quantities of protein (10–1000 µg) were chromatographed on analytical columns (Keystone Scientific Betabasic-8 and Deltabond octyl; both 250 × 4.6 mm i.d., 5 µm particle size, 100 Å pore size) at a flow-rate of 1 ml min⁻¹. Columns were equilibrated in degassed water–acetonitrile–TFA (95 : 5 : 0.1) and eluted with the same increasing linear gradient of degassed 0.1% TFA in acetonitrile over 215 mins (time/% acetonitrile = 0/5, 10/40, 210/60, 215/100). Loadings of up to 1 mg of protein per run for analytical columns were tolerated without compromising the separation of various isoforms. The two different types of packings used for the analytical columns gave essentially identical separations. The eluate absorbance was monitored at 215 and 280 nm, and immediately upon collection fractions were placed in a vacuum centrifuge for rapid removal of acetonitrile. Subsequently, the remaining solvent was removed by lyophilization. The dried fractions were weighed and stored at -80 °C. The dried fractions were brought to room temperature and samples were removed, weighed and redissolved in solvents and buffers as noted for further characterization.

Guanidine–DTT-treated CSAct was desalted without attempting isoform resolution by C₄ RP-HPLC (Vydac, Hesperia, CA, USA; 10 µl particle size, 300 Å pore diameter, 250 × 4.6 mm i.d.) in which the column was equilibrated in water–acetonitrile–TFA (95 : 5 : 0.1) and eluted (1 ml min⁻¹) with an increasing linear gradient (1.58% min⁻¹) of 0.1% TFA in acetonitrile over 60 min. Column loadings of up to 1 mg of protein per run were used. The eluate absorbance was monitored at 215 and 280 nm and the peak eluting between 50 and 65% acetonitrile was collected and treated as described above for the other HPLC fractions.

Preparation of CSAct–CS complex

This was carried out as previously described²⁸ using a mixture of rat brain [³⁵S]CS plus bovine brain CS (50–150 nmol total CS containing 20 × 10³ cpm) or palmitoyl sulfatide (50–150 nmol) in 20 µl of chloroform or chloroform–methanol–water (66 : 33 : 5 v/v/v) which were dried in a stream of nitrogen. The dried residues were vigorously mixed with Tris–HCl buffer (25 mM, pH 7.5, 30 µl), then diluted with sodium acetate buffer (1 M, pH 4.5, 45 µl) to which was added a solution of CSAct protein (17–85 nmol in 200 µl of Tris–HCl, pH 7.5, 25 mM). The molar ratio of CS to CSAct was typically 3 : 1. The mixtures were incubated at 37 °C for 2 h following which they were loaded on a size-exclusion column (Ultragel AcA 34, LKB, Bromma, Sweden; 20 × 1.5 cm i.d., suspended in degassed 50 mM Tris–HCl pH 7.5). The column was eluted under gravity with suspension buffer (about 400 µl min⁻¹) and 20 l ml fractions were

collected. When [³⁵S]CS was used, the radioactivity content and OD₂₈₀ were determined for each collected fraction, and the peak fractions containing superimposable radioactivity and 280 nm absorption profiles were pooled (typically fractions 9–12), then dialyzed overnight against water, and the dialyzed preparation (about 4 ml) was dried either in a vacuum centrifuge or by lyophilization and stored at -4 °C. When palmitoyl-CS was used the elution position of the CS–CSAct complex was determined from the peak of 280 nm absorption with reference to the [³⁵S]CS-containing chromatograms. The dried samples were redissolved in water and aliquots diluted in other buffers as noted for examination by positive and negative ion ESI.

Electrospray mass spectrometry

A Perkin-Elmer SCIEX (Thornhill, ON, Canada) API III triple-quadrupole mass spectrometer fitted with an IonSpray source was tuned and calibrated as previously described.²⁹ Positive ion protein spectra were produced by injection of a solution typically in acetonitrile–water–formic acid (50 : 50 : 0.1 at 20 pmol µl⁻¹), although other solvents and concentrations were also used as noted (7–20 µl per injection) into a stream of the same solvent entering the ion source (10 µl min⁻¹), with the mass spectrometer scanning from *m/z* 1000 to 2000 (step size 0.3 Da, dwell time 2.0 ms, 6.14 s per scan, orifice voltage 90 V). Positive fragment ion spectra of Q1 pre-selected precursor ions were produced by scanning Q3 from 50 to 2400 (step size 1 Da, dwell time 3 ms, 7.18 s per scan, orifice voltage 110 V, collision gas (10% nitrogen in argon) thickness instrumental setting (CGT) of 208, R₀–R₂ offset of 50 V). Calculation of molecular masses from the series of multiply charged ions found in the protein spectra and deconvolution of the ion series into a molecular mass spectrum were achieved with the MacSpec computer program (version 3.3, Perlel-Elmer SCIEX). Calculation of theoretical peptide or protein average (chemical) molecular masses and prediction of fragment ion *m/z* values were achieved with the MacBiospec computer program (version 1.0.1, Perlel-Elmer SCIEX, based on the MacProMass computer program³⁰). The designations of Roepstorff and Fohlman³¹ and Biemann³² were used for describing collisionally induced protein fragment ions (b for N-terminal containing and y for C-terminal containing). CS spectra were produced in the negative ion mode from solutions of CS and CS–CSAct complexes in chloroform–methanol (1 : 1) and chloroform–methanol–water (66 : 33 : 5 v/v/v) by scanning from *m/z* 700 to 1000 (step size 0.3 Da, dwell time 6 ms c, 6.05 s per scan, orifice voltage -90 V).

Some samples were also analyzed on an electrospray/time-of-flight (ESI/TOF) mass spectrometer at the University of Manitoba.³³ This instrument has an effectively unlimited *m/z* range, so it can detect ions of high *m/z* that would be missed by the triple-quadrupole instrument. Two electrospray sources were used. A conventional ESI source with a flow-rate of ~0.2 µl min⁻¹ was used for samples dissolved in aqueous ammonium acetate buffer with concentrations up to about 20 mM and a nanospray source³⁴ was used for higher buffer concentrations of up to 100 mM.

Measurement of protein concentrations

CSAct concentrations were estimated from the OD₂₈₀ using an extinction coefficient of 5×10^3 (mol⁻¹ cm⁻¹). This was determined from the OD₂₈₀ of samples that had been subjected to quantitative amino acid analysis (UCLA Microprotein Sequencing Facility). CSAct concentrations were also measured by the Lowry procedure using BSA as standard. On a mg ml⁻¹ basis, the Lowry-based and OD₂₈₀-based CSAct concentration estimates were the same.

RESULTS

Native pig kidney CSAct

ESI mass spectra revealed the expected series of ions corresponding to the 1-, 2-, 4- and 5-CHO isoforms previously reported³⁵ (Fig. 1(A) and 1(C), which

accounted for 79% of the *m/z* 1000–2000 reconstructed ion current profile (Table 1). There were also present several series of less intense signals, the structures of which could be reasonably rationalized on the basis of the molecular mass measurements. One of these series appeared as upfield satellites riding on the shoulder of each main ion with molecular masses which averaged 15 Da greater than each corresponding main signal. These signals most likely reflect oxidation of a single methionine residue.²⁷ Their intensity was typically only 1–3% of each corresponding main signal, although this increased in protein preparations that had been stored frozen for long periods of time and in samples that had been left in solution at room temperature unprotected from atmospheric oxygen. An analogous but even less intense series of signals could also be detected after scale expansion in the original spectra and appear at about 32 Da heavier than each corresponding main signal. These most likely result from inclusion of an additional oxygen atom. Not unexpectedly, this series of ions also became more prominent in samples that had been given

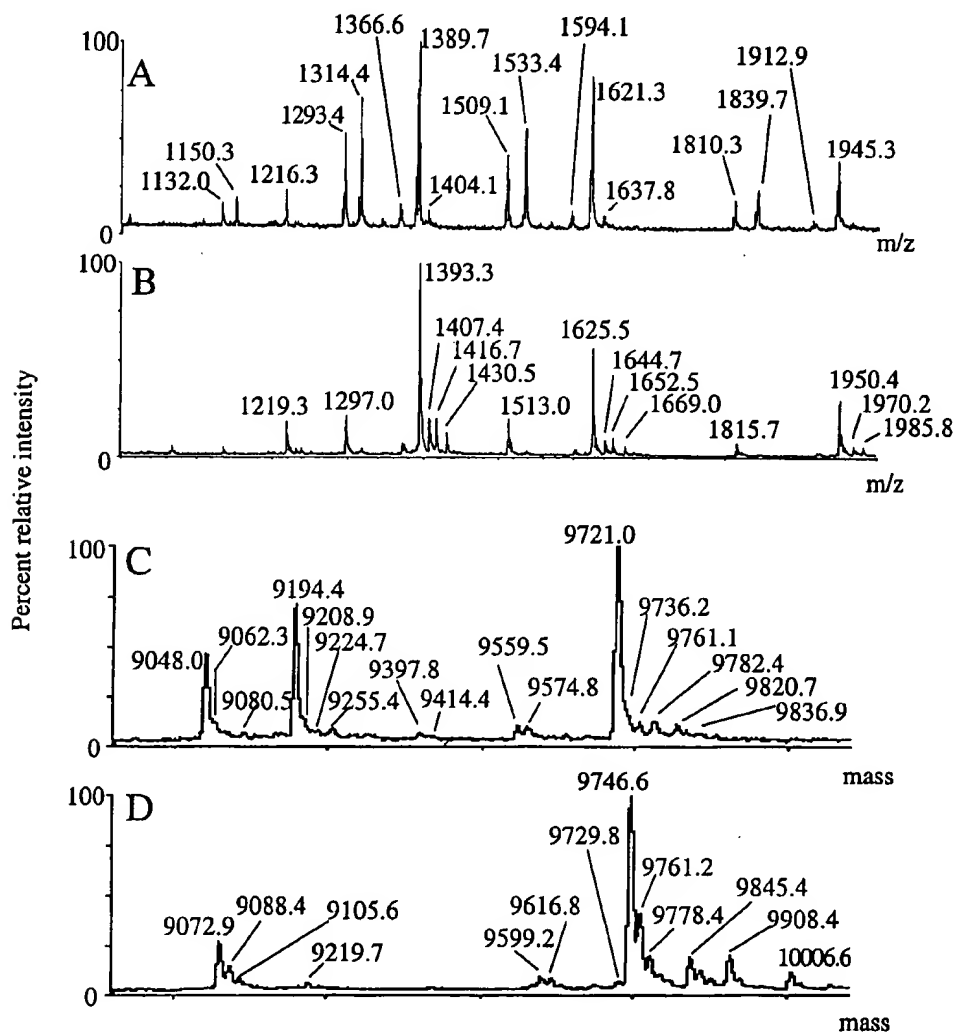


Figure 1. Electrospray ionization mass spectra of native pig kidney (A) and native human urine (B) CSAct, and the corresponding Hypermass reconstructed molecular mass profiles (C and D, respectively). The samples were dissolved in water–acetonitrile–formic acid (50:50:0.1) at 20 pmol μl^{-1} and 20 μl were injected into the ion source for the collection of the spectra.

Table 1. ESI-identified components of pig kidney CSAct

Observed molecular mass	Probable identity	Calculated molecular mass	Difference (measured - calculated)	Relative signal intensity ^a	% total ion current ^a
Native protein^a					
9048.0	1CHO	9047.4 ^c	+0.6	45.3	16.1
9062.3	1CHO + 14.3 Da			2.9	1.0
9080.5	1CHO + 32.5 Da			1.8	0.6
9110.0	1CHO + 62.0 Da			3.4	1.2
9194.4	2CHO	9193.6 ^d	+0.8	69.8	24.7
9208.9	2CHO + 14.5 Da			3.3	1.2
9224.7	2CHO + 30.3 Da			2.4	0.9
9231.8	2CHO + 37.4 Da			2.9	1.0
9255.4	2CHO + 61.0 Da			4.5	1.6
9293.7	2CHO + Val ₈₀	9292.7 ^e	+1.0	2.4	0.9
9397.8	3CHO	9396.8 ^f	+1.0	3.7	1.3
9559.5	4CHO	9558.9 ^g	+0.6	7.2	2.6
9574.8	4CHO	9574.9 ^h	-0.1	6.8	2.4
9721.0	5CHO	9721.0 ⁱ	0.0	100.0	35.4
9736.2	5CHO + 15.2 Da			1.1	0.4
9754.2	5CHO + 33.2 Da			2.2	0.8
9761.1	5CHO + 40.1 Da			5.6	2.0
9782.4	5CHO + 61.4 Da			7.2	2.6
9820.7	5CHO + Val ₈₀	9820.2 ^j	+0.5	6.2	2.2
9837.0	5CHO + Val ₈₀ + 16.3 Da			3.4	1.2
Deglycosylated protein^b					
8585.8	0CHO ₁₋₇₇	8587.0 ^k	-1.2	2.2	1.9
8844.9	0CHO	8845.2 ^l	-0.3	100.0	84.7
8882.8	0CHO + 37.9 D			8.2	6.9
8944.3	0CHO + Val ₈₀	8944.3 ^m	0	7.7	6.5

^{a,b} Samples were prepared ^awithout and ^bwith RP-HPLC purification, and injected into the ESI ion source at 20 pmol μl^{-1} of water-acetonitrile-formic acid (50:50:0.1).

^{c-m} Molecular masses were calculated after inclusion of ^cHexNAc; ^dHexNAcdHex; ^eVal₈₀-CSAct₁₋₈₀ with HexNAcdHex; ^fHexNAc₂dHex; ^gHexNAc₂HexdHex; ^hHexNAc₂Hex₂; ⁱHexNAc₂dHex; ^jVal₈₀-CSAct₁₋₈₀ with HexNAc₂dHex; ^kAsp₂₁-CSAct₁₋₇₇; ^lAsp₂₁-CSAct₁₋₇₉; and ^mVal₈₀-Asp₂₁-CSAct₁₋₈₀.

^a Estimated from the relative signal intensities in the Hypermass reconstructed molecular mass profiles [Fig. 1(C)]. Excluding components estimated as <1% of the main component.

the opportunity for reaction with atmospheric oxygen. Not recognized in earlier work is the presence of a molecule 99–100 Da heavier than the main signal. This isoform is always evident in association with the 5CHO glycoform where it represents on average 5–10% of the predominant 5CHO₁₋₇₉ component. A corresponding component is also seen with 2–3% relative abundance associated with the 2CHO glycoform (Table 1). These are probably due to the presence of a valine at position 80 of the protein (valine residue mass = 99.1 Da), which would be consistent with the prediction based on the human,^{18–20} rat,³⁶ mouse³⁷ and chicken³⁸ cDNA sequences. Another minor component in native PKA is an additional 4CHO glycoform assigned here as two *N*-acetylhexosamine plus two hexose moieties (HexNAc₂Hex₂, Table 1). While this glycoform is isomeric with the mono-oxidized form of the *N*-acetylhexosamine (2) + hexose (1) + deoxyhexose (1) 4CHO glycoform (HexNAc₂HexdHex) previously recognized,³⁵ distinction between inclusion of oxygen and substitution of a hexose for a deoxyhexose (both resulting in mass increments of 16 Da) is made on the basis of the equivalent relative intensity of the two signals which are inconsistent with the levels of mono-oxidation seen for the other glycoforms. Also, weak signals corresponding to molecules on average 37–40 and 61–62 Da heavier than the main signal are also evident in the spectra, but their masses are incongruent with common protein adducts

or other carbohydrate groups. Some samples of native PKA contained yet another series of ions 4 on average which were 15–16 Da lighter than the corresponding main signals. The occurrence of this ion series was variable, but was found to represent up to 33% of the main signal in an isolated case. The origin of the mass loss is obscure. Formation of an internal ester during protein purification is an attractive hypothesis to account for this ion series, but this would result in loss of 18 Da, which appears significantly greater than the measured mass loss. These signals were absent in the spectra of HPLC-purified deglycosylated protein (see below).

The chromatograms from extended C₈ RP-HPLC of PKA largely reflect the composition of the samples seen by ESI. The UV absorption profile of the chromatogram was dominated by a trio of peaks eluting between 43 and 44% acetonitrile which were characterized on the basis of ESI-measured molecular masses as principally due to the 1-, 2- and 5CHO isoforms [Fig. 2(A1)]. The less intense series of earlier eluting UV-absorbing peaks had measured molecular masses 16 or 32 Da higher, consistent with the presence of methionine oxidized isoforms. The UV-absorbing complex eluting before 20 min was a regular contaminant of the native preparations. ESI analysis of these fractions did not yield a significant ion current and no ion series characteristic of a protein. The area of the entire CSAct complex of peaks, including those due to

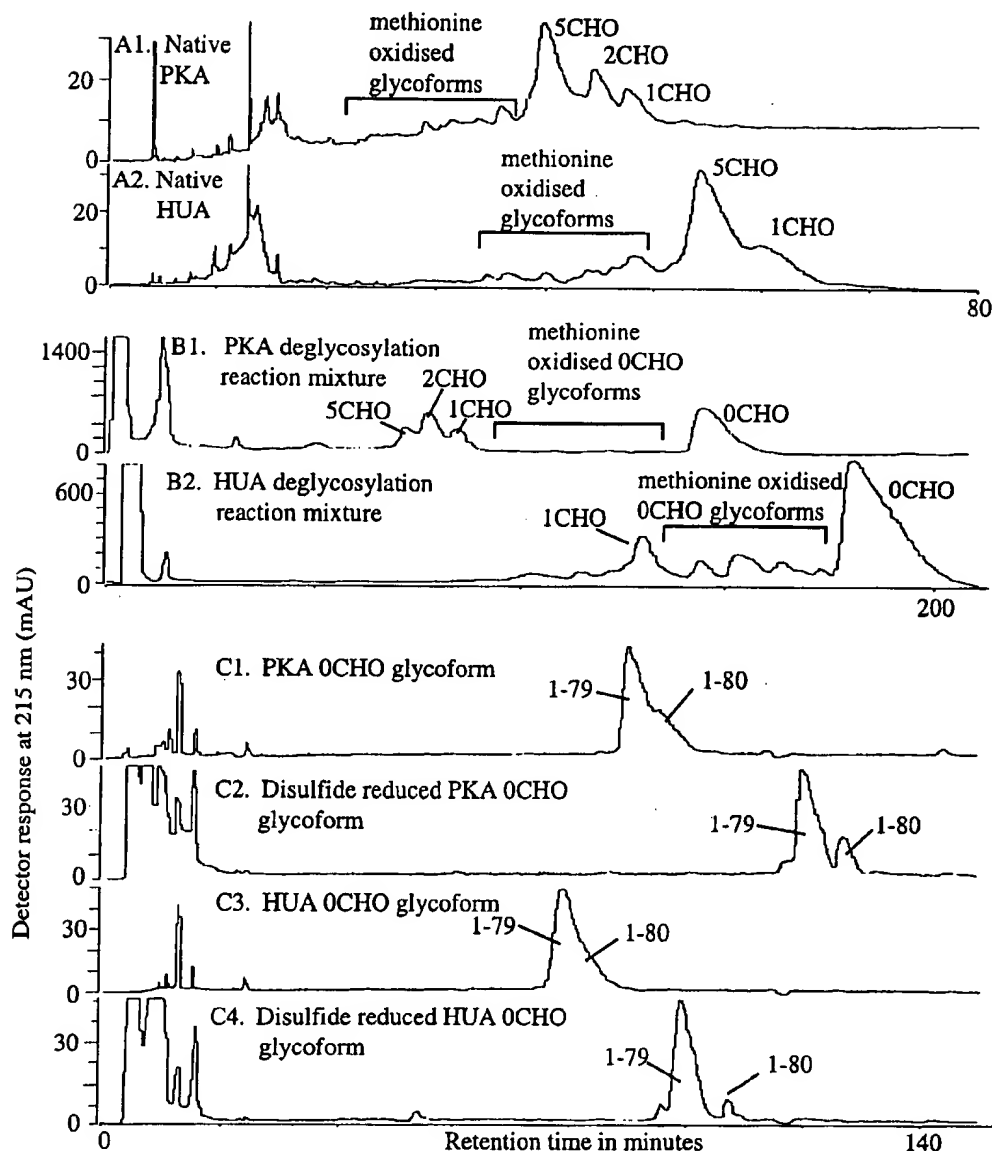


Figure 2. CSAc C₈ RP-HPLC 215 nm elution profiles: (A) native pig kidney (A1) and native human urine (A2) CSAc elution profiles from an analytical column (64.9 µg protein loaded in each); (B) PNGase F reaction mixtures of native pig kidney (B1) and native human urine (B2) CSAc elution profiles from a semi-preparative column (27 and 7 mg protein loaded, respectively); (C) deglycosylated (0CHO) native pig kidney (C1 and C2) and native human urine (C3 and C4) CSAc elution profiles from an analytical column (64.9 µg protein loaded for each chromatogram) without further treatment (C1 and C3) and after disulfide reduction (C2 and C4). Isoform assignments were made on the basis of molecular mass measurements (Tables 1 and 2).

the oxidized isoforms, was estimated to account for about 78% of the total 215 nm absorption profile.

Native human urine CSAc

ESI mass spectra revealed an analogous series of ions to those seen for native PKA, but in this case the spectra were dominated by ions derived from the 1-, 4- and 5CHO glycoforms²⁵ [Fig. 1(B) and 1(D)] which accounted for about 44% of the *m/z* 1000–2000 reconstructed ion current profile (Table 2). An accompanying series of less intense signals derived from molecules containing one and two additional oxygen atoms were also evident. These

were more intense than in the PKA spectra, accounting for up to 40% of each corresponding main component (Table 2). The assigned Val80 isoform represents about 11% of the *m/z* 1000–2000 ESI ion current. This is about the same intensity as found for PKA and twofold lower than the 1–79 residue protein previously reported for that isolated from human kidney.³⁹ The assigned 6CHO glycoform is on average 162 Da heavier than the 5CHO glycoform and probably represents the inclusion of an additional hexose which represents about 12% of the ion current. The presence of a 6CHO glycoform was unexpected in the preparation employed in this study since the purification scheme employed a Con A Sepharose

Table 2. ESI-identified components of human urine CSAct

Observed molecular mass	Probable identity	Calculated molecular mass	Difference (measured – calculated)	Relative signal intensity ^a	% total ion current ^a
Native protein^a					
9072.9	1CHO	9072.5 ^c	+0.4	24.6	8.6
9088.4	1CHO + 15.5Da			11.9	4.2
9105.6	1CHO + 32.7Da			5.2	1.8
9219.7	2CHO	9218.6 ^d	+1.1	3.3	1.2
9583.3	4CHO	9584.0 ^e	-0.7	1.9	0.7
9599.2	4CHO	9600.0 ^f	-0.8	5.6	2.0
9616.8	4CHO + 17.6			5.2	1.8
9729.8	5CHO – 16.8Da			4.4	1.5
9746.6	5CHO	9746.1 ^g	+0.5	100.0	35.0
9761.2	5CHO + 14.6Da			39.3	13.8
9778.4	5CHO + 32.2Da			17.0	5.9
9845.4	5CHO + Val ₈₀	9845.2 ^h	+0.3	17.0	5.9
9860.4	5CHO + Val ₈₀ + 15Da			9.6	3.4
9878.6	5CHO + Val ₈₀ + 33.2Da			5.9	2.1
9908.4	6CHO	9908.3 ⁱ	+0.1	17.8	6.2
9923.8	6CHO + 15.4D			5.2	1.8
1006.6	6CHO + Val ₈₀	10007.4 ^j	-0.8	8.9	3.1
10022.6	6CHO + Val ₈₀ + 16Da			3.0	1.0
Deglycosylated protein^b					
8740.8	0CHO ₁₋₇₈	8741.2 ^k	-0.4	4.4	3.2
8868.6	0CHO	8870.3 ^l	-1.7	100.0	72.0
8887.3	0CHO + 18.7Da			10.4	7.5
8908.4	0CHO + 39.8Da			17.0	12.2
8968.0	0CHO + Val ₈₀	8969.4 ^m	-1.4	7.1	5.1

^{a,b} Samples were ^awithout and ^bwith RP-HPLC purification, and injected into the ESI ion source at 20 pmol µl⁻¹ of water–acetonitrile–formic acid (50:50:0.1).

^{c–m} Molecular masses were calculated after inclusion of ^cHexNAc; ^dHexNAcHex; ^eHexNAcHexdHex; ^fHexNAcHex₂; ^gHexNAcHex₂dHex; ^hVal₈₀–CSAct₁₋₇₉ with HexNAcHex₂dHex; ⁱHexNAcHex₃dHex; ^jVal₈₀–CSAct₁₋₈₀ with HexNAcHex₃dHex; ^kAsp₂₁–CSAct₁₋₇₈; ^lAsp₂₁–CSAct₁₋₇₉; and ^mVal₈₀–Asp₂₁–CSAct₁₋₈₀.

^a Estimated from the relative peak heights in the Hypermass reconstructed molecular mass profiles [Fig. 1(D)]. Excluding components estimated as <1% of the main component.

chromatographic step. It is felt that this indicates failure of the Con A Sepharose lectin affinity step in the purification of this sample of protein.²⁵ The spectra also revealed the presence of a small amount of a 2CHO glycoform, representing only 1.1% of the ion current, and signals assigned as being from two different 4CHO glycoforms representing the previously recognized²⁵ HexNAc₂ HexdHex and a HexNAc₂ Hex₂ glycoform. As with the interpretation of the PKA spectra, distinction between inclusion of oxygen and substitution of hexose for deoxyhexose are made on the basis of the relative intensity of the two signals which are inconsistent with the levels of mono-oxidation seen for the other glycoforms.

The RP-HPLC trace from native HUA was dominated by a single peak and a partially resolved shoulder eluting between 44 and 46% acetonitrile which were characterized on the basis of ESI-measured molecular masses as principally due to the 1- and 5CHO isoforms [Fig. 2(A2)]. Again the less intense series of earlier eluting UV-absorbing peaks had measured molecular masses 16 or 32 Da higher, consistent with the presence of methionine-oxidized isoforms. The UV-absorbing complex eluting before 20 min was a regular contaminant of the native HUA preparations. The area of the entire CSAct complex of peaks, including the those due to the oxidized isoforms, accounted for about 77% of the total 215 nm absorption profile.

Deglycosylation of native CSAct

Extended RP-HPLC of PKA and HUA PNGase F reaction mixtures on a semi-preparative scale revealed in order of elution residual 5-, 2- and 1CHO glycoforms, methionine-oxidized 0CHO isoforms²⁷ and lastly the deglycosylated protein [Fig. 2(B1) and (B2)]. In some deglycosylation reactions the residual 5CHO glycoform was below the limits of detection at the time the reaction was arrested. The increased abundance of oxidized methionine isoforms in HUA compared with PKA is reflected in the relative intensity of the UV HPLC traces. ESI analysis of the HPLC-purified deglycosylated materials showed the measured molecular mass of the main component to be consistent with what would be expected for each apoprotein with an Asp substituted for Asn at position 21 following the deglycosylation reaction (Fig. 3, Tables 1 and 2). The presence of Asp at position 21 was confirmed in the case of PKA by automated Edman sequencing (data not shown).

The PKA-derived material also revealed the presence of a weak signal tentatively assigned as being derived from the Asp₂₁–apoprotein₁₋₇₇ sequence, for which retrospective searches in native PKA were negative, a weak signal for a molecule 38 Da heavier than the main component and a signal for the Val₈₀ isoform. The HUA-derived material revealed the presence of a weak signal tentatively assigned as being derived from the Asp₂₁–apoprotein₁₋₇₈

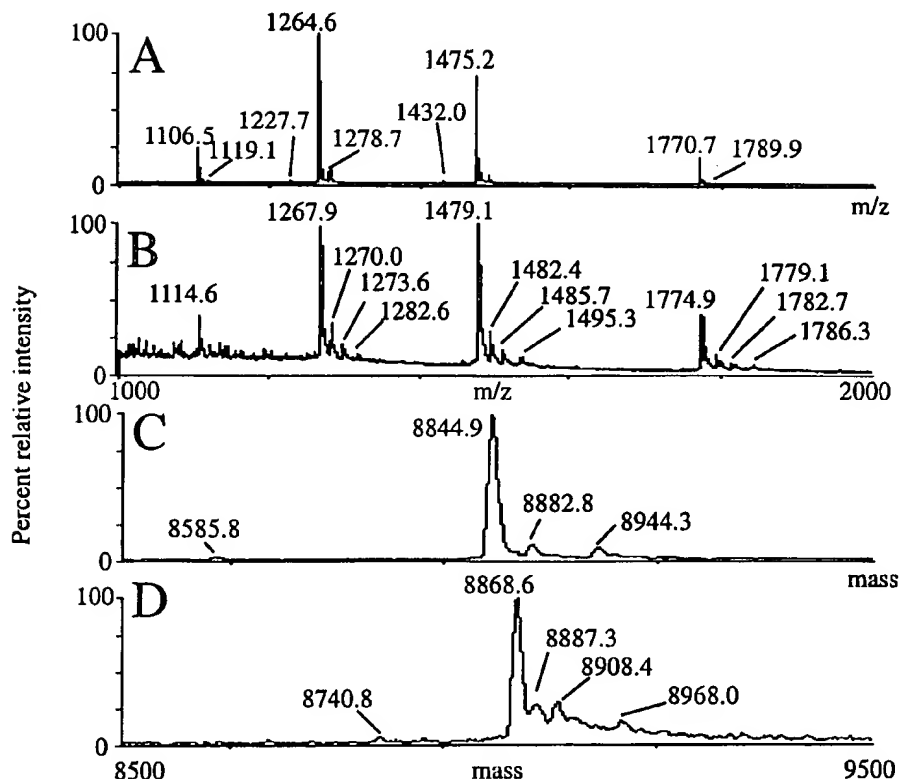


Figure 3. Electrospray ionization mass spectra of deglycosylated pig kidney (A) and human urine (B) CSAc and the corresponding Hypermass reconstructed molecular mass profiles (C and D, respectively). The spectra were collected from 20 pmol μL^{-1} protein solutions in water–acetonitrile–formic acid (50:50:0.1).

sequence, for which retrospective searches in native HUA were negative, weak signals for molecules 19 and 40 Da heavier than the main component and a signal for the Val₈₀ isoform. The results suggests the presence of a small amount of carboxypeptidase activity during the deglycosylation reaction resulting in the loss of one or two carboxyl-terminal amino acid residues from HUA and PKA, respectively. Apparently these truncated molecules were not separated from the main component even after extended RP-HPLC. The combined 1–79 plus 1–80 components in the OCHO fraction accounted for 91 and 77% of the ESI ion current for the PKA and HUA samples, respectively. No detectable amount of oxygen-adducted species were evident in the spectra, and the structures of the 19 and 38–40 Da adducts are obscure.

Rapid removal of the volatile components of the the HPLC eluate permitted the preservation of biological activity. Actually it was possible to maintain the material for several hours in water–acetonitrile–TFA (50:50:0.1) with no discernible effect on the ability of the protein to support arylsulfatase A-catalysed sulfate hydrolysis from CS. However, ESI analysis of one deglycosylation reaction mixture in which the fractions from C₈ RP-HPLC purification were stored at -80°C before vacuum concentration and lyophilization showed dramatically different spectra to that shown in Fig. 3(A). In this experiment the ESI spectra of the deglycosylated protein revealed a pattern of broad, regularly spaced recurring signals of decreasing intensity with the same charge state distribution as that shown in Fig. 3(A). Calculations showed

the predominant molecule to be about 24 Da lighter than expected (8821 Da) and each satellite species was about 38 Da heavier. One explanation for this result is the acid halide-catalyzed formation of imido esters.^{40,41} Irrespective of the actual mechanism, exhaustive dialysis against water resulted in disappearance of these adducts and the reappearance of the expected mass spectrum and expected molecular mass. The biological activity of the dialyzed protein was undiminished. The formation of these adducts did not appear when the RP-HPLC fractions were subjected to vacuum concentration followed by lyophilization immediately following collection.

Rechromatography of the OCHO glycoforms on an analytical scale produced 215 nm profiles virtually identical with those obtained with the semi-preparative columns in which the 1–80 isoforms were not separated from the 1–79 components and eluted on the trailing edge of the predominant isoforms [Fig. 2(C1) and (C3)]. However, on the analytical column and under the same conditions the disulfide-reduced preparations had longer retention times and sharper peaks, which resulted in baseline separation of the 1–79 and 1–80 isoforms [Fig. 2(C2) and (C4)].

Effect of solvation conditions on the ESI spectra

When dissolved in 0.1% TFA (pH 2), the ESI spectra of CSAc were dominated by the pentuply charged ions [Fig. 4(C)]. On the other hand the spectra were dominated by the heptuply charged ions when the protein was dissolved in either 0.1% formic [Fig. 4(A)] or 2% acetic

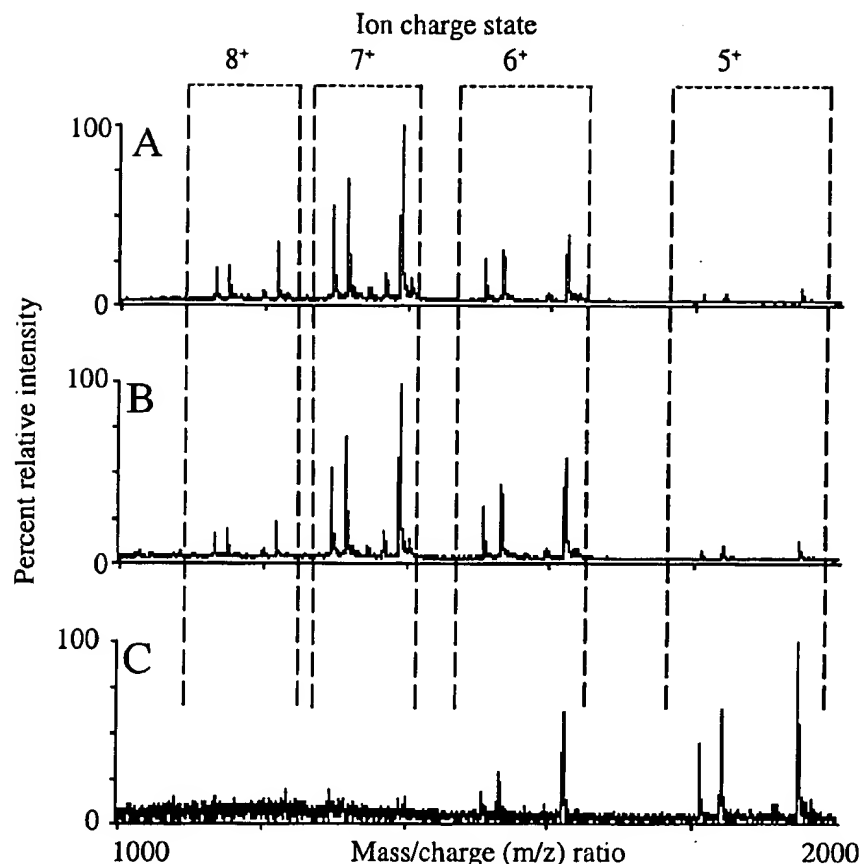


Figure 4. Comparison of the electrospray mass spectra of pig kidney CSAcT from solutions of water–acetonitrile (50:50) containing (A) 2% acetic acid (pH 2.6), (B) 0.1% formic acid (pH 2.8) and (C) 0.1% TFA (pH 1.9), all at a concentration of 20 pmol μL^{-1} . The samples were prepared and the spectra recorded as described for Table 3.

acid [Fig. 4(B)] at pH 2.76 and 3.21, respectively. Substitution of formic or acetic acid for TFA increased the signal intensity by a factor of 9–13 (Table 3). The spectral patterns were uninfluenced by the inclusion of acetonitrile in the solvent, although this did result in further significant increases in signal intensity of 2–3-fold with the formic and acetic acid-containing samples (Table 3). Further increase in the acetic acid concentration to 4% had no effect on the spectral pattern although the signal intensity was decreased by a factor of 4.2. Dilute solutions of ammonium acetate at pH 4.32 and 6.06, with or without the addition of acetonitrile, greatly diminished the ESI response from the protein to a barely detectable level, and virtually no response was obtained when the protein was dissolved in water at around pH 6 (Table 3). Protein in which the disulfide bonds were reduced gave the same spectral pattern with the heptuply charged ions predominating, and similar signal intensities, when solvated in water–acetonitrile mixtures containing either 0.1% formic or trifluoroacetic acid (Table 3).

MS/MS

The most significant ions created from collisionally induced dissociation of the pentuply charged precursor ions of the 5CHO glycoform from native PKA resulted

from molecular mass decrements that matched the residue masses for dHex, dHexHex, dHexHex₂ and HexNAcHex₂ dHex, with the simultaneous appearance of the quadruply charged forms of these fragment ions [Fig. 5(C)]. This spectrum also revealed the appearance of weak fragment ions at m/z 528 and 366 which are rationalized as being due to singly protonated HexNAcHex₂ and HexNAcHex fragments, respectively, and more abundant fragment ions in the low- m/z region at 204, 186, 168 and 138 which are probably to be due to the singly protonated individual sugar residues and fragments thereof. A similar but simpler array of fragment ions emerged from tandem mass spectrometry (MS/MS) of the pentuply charged parent of the 2CHO glycoform in which simple loss of a deoxyhexose was seen with the appearance of the corresponding quadruply charged ion and a weak signal for the free HexNAc residue [Fig. 5(B)]. Under the same conditions there were no significant high- m/z fragment ions formed from the pentuply charged parent of the 1CHO glycoform, although this spectrum revealed a weak signal at m/z 204 corresponding to the HexNAc residue [Fig. 5(A)]. Virtually identical spectra were obtained from the pentuply charged precursor ions from the 1-, 2- and 5CHO glycoforms from disulfide-reduced protein with one minor exception, namely the formation of a weak fragment ion at m/z 1410 [Fig. 5(D)]. This ion was formed

Table 3. Effect of solvation conditions on pig kidney CSAc ESI spectral characteristics

Solvent	Buffering ion concentration (mM)	pH	Dominant charge state	Relative signal intensity
<i>Native protein^a</i>				
Water-TFA, 100:0.1	13.4	1.9	5	2.9
Water-acetonitrile-TFA, 50:50:0.1	13.4		5	2.0
Water-formic acid, 100:0.1	23.4	2.8	7	23.2
Water-acetonitrile-formic acid, 50:50:0.1	23.4		7	71.3
Water-acetic acid, 100:0.1	17.4	3.2	7	35.9
Water-acetic acid, 100:2	348	2.6	7	33.3
Water-acetonitrile-acetic acid, 50:50:2	348		7	100
Water-acetic acid, 100:4	696	2.5	7	23.8
Aqueous ammonium acetate	2.5	4.3		<1
Aqueous ammonium acetate-acetonitrile, 50:50	2.5			<1
Aqueous ammonium acetate	5	4.3		<1
Aqueous ammonium acetate	5	6.1		<1
Water		6.0		<1
<i>Disulfide-reduced protein^b</i>				
Water-acetonitrile-TFA, 50:50:0.1	13.4		7	NA ^c
Water-acetonitrile-formic acid, 50:50:0.1	23.4		7	NA

^a Native PKA in Tris-HCl (25 mM, pH 7.5) was exhaustively dialyzed (3.5 kDa molecular mass cut-off) against water then lyophilized to dryness. The dried protein was redissolved in the indicated solvents to 20 pmol μL^{-1} and injected (20 μL) into a stream of the same solvent entering the mass spectrometer source (10 $\mu\text{L min}^{-1}$). The average of all the spectra accrued from each injection was computed and the relative signal intensity (average of two separate experiments) was estimated from the intensity of the signal for the 5CHO isoform in the Hypermass reconstructed spectra.

^b Disulfide-reduced PKA was prepared as described in the Experimental section and desalted by C_4 RP-HPLC. The dried HPLC fractions were redissolved in the solvents indicated and injected into a stream of the same solvent entering the mass spectrometer source.

^c NA, data not available.

from all glycoforms and without further information was nominally assigned as possibly due to either the b_{13}^+ or y_{13}^+ fragment ion.

Monomeric and polymeric states of CSAc and CS-CSAc complexes

CS-CSAc complexes were prepared with both native PKA and the HPLC purified 0CHO isoform using mixed rat-bovine brain CS and synthetic palmitoyl-CS. Material recovered from the size-exclusion column revealed strong signals during ESI for the protein in the positive ion mode and for CS in negative ion mode. Searches were made for the presence of CS-CSAc complexes, and for polymeric forms of CSAc protein, in the gas phase during positive ion ESI with the triple-quadrupole instrument (m/z range <2400) using the conventional IonSpray source. Various solvents were used including water-acetonitrile-formic acid (50:50:0.1), water-formic acid (100:0.1), water-acetic acid (100:0.1, 100:0.01, 100:0.05) and aqueous ammonium acetate (5–10 mM, pH 4.5). Other instrumental parameters were adjusted to maximize the likelihood of retaining non-covalent complexes in the gas phase. This involved reducing the orifice voltage, reducing the quadrupole offset voltages (instrumental settings of R_0 – R_3 were used with differences of 3, 2, 1 and 0.5 V) and lowering the interface temperature from the normal setting of 55°C to 39, 33 and 26°C. Samples were analyzed concurrently with horse heart myoglobin. Using a low quadrupole offset voltage, the molecular mass of horse heart myoglobin was measured at 17 568.0 Da from

solutions of dilute acetic acid, reflecting retention of heme on the apoprotein. These spectra revealed smaller and varying amounts of the apoprotein at a molecular mass of 16951 Da. With a quadrupole offset voltage of 0.5 V the apoprotein was not evident in the spectra. Under identical conditions, native and 0-CHO PKA revealed strong signals for monomeric protein with no evidence for dimeric forms of the protein. Lowering the interface temperature and the orifice voltage had no apparent effect on this result. Under the same conditions, CS-CSAc complexes gave no evidence for the presence of gas-phase ions corresponding to two molecules of protein plus one molecule of CS. However, from solutions of dilute formic acid and water-acetonitrile-formic acid, the CS-CSAc complex preparations revealed ions corresponding to molecules of molecular masses 9737 and 9626 Da from preparations made with rat/bovine brain CS and palmitoyl-CS, respectively [Fig. 6(A) and (B)]. These measurements agree with that which would be derived from one molecule of protein (calculated molecular mass for the 0CHO isoform of 8845.2 Da) and one molecule of palmitoyl-CS (calculated molecular mass of 780.1 Da) or one molecule of the c24:1 CS isoform (calculated molecular mass 890.3 Da, the predominant CS isoform in the rat/bovine brain CS preparation used^{42,43}). The maximum intensity of the ions for the CS-protein complex was less than 25% of those from the naked protein in the same spectra, recorded with an orifice voltage of 80 V, an interface temperature of 39°C and a quadrupole offset voltage of 1 V and with the preparation dissolved in 0.05% formic acid.

Similar samples were run on the ESI TOF mass spectrometer in aqueous ammonium acetate solution at

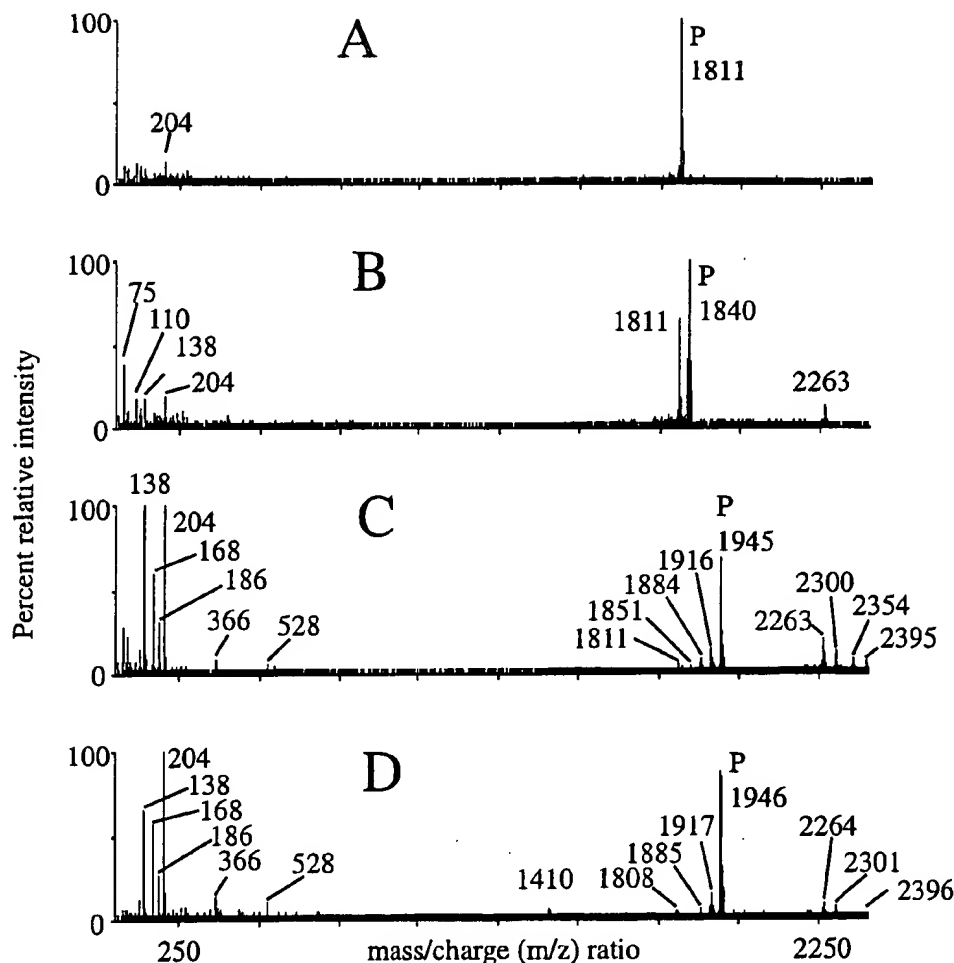


Figure 5. Tandem mass spectra of native (A, B and C) and disulfide-reduced (D) pig kidney CSA. P = parent ion and in each case is the pentuply charged ion from the (A) 1-, (B) 2- and (C and D) 5CHO CSA₁₋₇₉ glycoforms, respectively. Nominal assignments of the fragment ions: m/z 1917, 1916 and 1811 all assigned as loss of dHex (observed mass loss = 145 Da, calculated = 146 Da); m/z 1888 and 1884 both assigned as loss of dHexHex (observed mass loss = 305 Da, calculated = 308 Da); m/z 1851 assigned as loss of dHexHex₂ (observed mass loss = 470 Da, calculated = 470 Da); m/z 1808 and 1811 both assigned as loss of HexNAcHexHex₂ (observed mass loss = 675 Da, calculated = 674 Da); m/z 2396, 2395 and 2263 assigned as quadruply charged versions of m/z 1917, 1916 and 1811, respectively; m/z 2354 assigned as quadruply charged version of m/z 1884; m/z 2264 and 2263 assigned as quadruply charged versions of m/z 1808 and 1811, respectively; m/z 2301 and 2300 assigned as (2CHO-CSA₁₋₇₉)⁴⁺ (calculated m/z = 2300.9 and 2299.4 for disulfide-reduced and disulfide-oxidized forms, respectively); m/z 528 assigned as HexNAc₁Hex₂ (calculated residue mass = 527.5); m/z 366 assigned as HexNAcHex (calculated residue mass = 365.3); m/z 204 assigned as HexNAc (calculated residue mass = 203.2); m/z 1410 assigned as b_{13}^{+} or y_{13}^{+} (calculated m/z = 1409.6 and 1410.7 Da, respectively).

pH 4.5–6. The spectra of the protein samples measured with conventional electrospray at low buffer concentration (5–10 mM) revealed strong signals for the monomeric protein with progressively smaller amounts of dimer, trimer and tetramer at higher m/z values, suggesting that these result from non-specific binding. The spectra of the protein–palmitoyl-CS complex in 5–10 mM buffer again contained the protein monomer as the dominant species, but a complex of the monomer with one molecule of attached lipid (as seen above) was present at ~20% of the signal intensity of the monomeric protein. At still lower intensity (a few percent), signals were recorded consistent with a single charge state of the species: [monomer + 2 lipids] (5+), dimer (7+), and [dimer + 1 lipid] (7+).

Dramatically different spectra were observed when the protein–palmitoyl-CS complex was examined with

nanospray in 100 mM ammonium acetate buffer [Fig. 6(C)]. At a declustering voltage of 105 V the peaks were particularly broad, presumably because of the presence of multiple adducts, but signals corresponding to the dimer and the [dimer + 1 lipid] were present at an intensity comparable to those for the monomer ions. At higher declustering voltages the relative intensity of the dimer and [dimer + 1 lipid] ions decreased until they disappeared at a declustering voltage of 185 V, leaving only monomer ions and ~20% [monomer + 1 lipid] ions.

DISCUSSION

ESI mass spectrometry in combination with extended C₈ RP-HPLC has allowed the description of the components

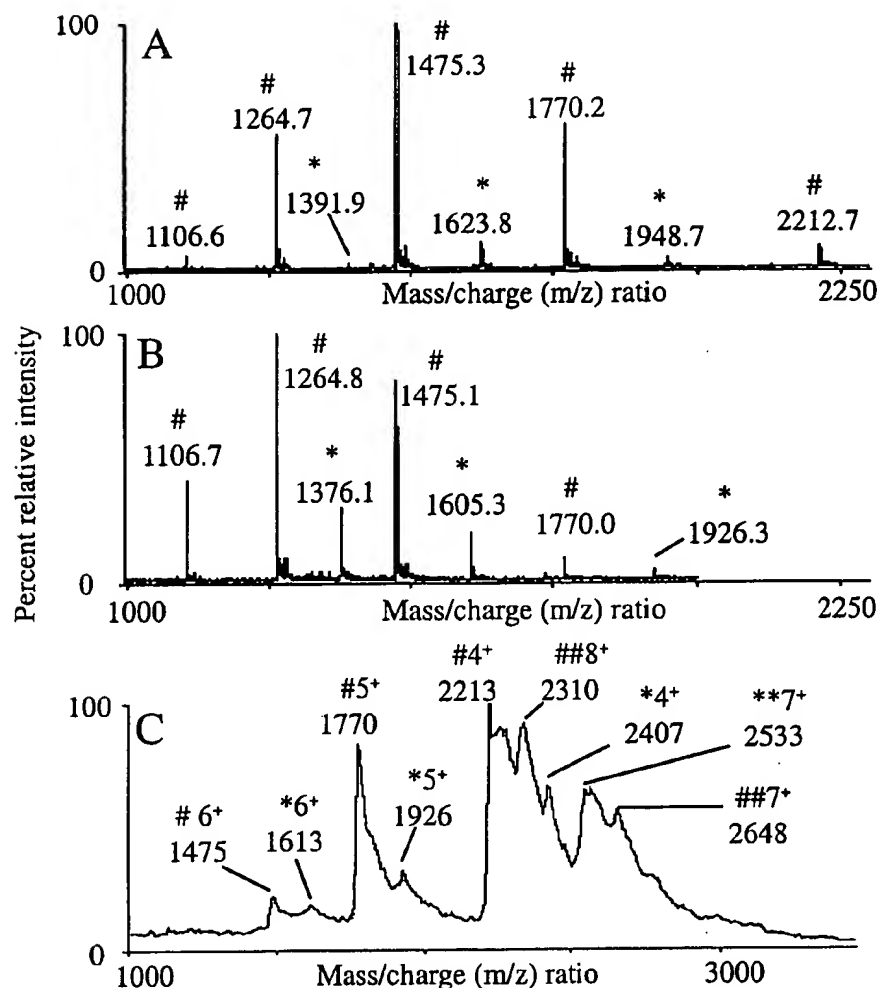


Figure 6. Electrospray ionization mass spectra of CSAct-CS complexes collected as described in the text. (A) 0CHO CSAct-rat/bovine CS complex observed with an IonSpray source from a solution in $\text{CH}_3\text{CN}-\text{H}_2\text{O}-\text{HCOOH}$ (50:50:0.1). *Three estimates of compound mass gave a mean result of 9737.2 Da; #four estimates of compound mass gave a mean result of 8845.8 Da. (B) 0CHO CSAct-palmitoyl-CS complex observed with an IonSpray source from a solution in $\text{CH}_3\text{CN}-\text{H}_2\text{O}-\text{HCOOH}$ (50:50:0.1). *Three estimates of compound mass gave a mean result of 9626.0 Da; #four estimates of compound mass gave a mean result of 8845.0 Da. (C) 0CHO CSAct-palmitoyl-CS complex observed with a nanospray source from a solution in 100 mM ammonium acetate (pH 4.5) at a declustering voltage of 105V. #Correspond to CSAct monomer; *correspond to CSAct monomer + lipid; ##correspond to CSAct dimer + lipid; **correspond to CSAct dimer.

of PKA and HUA with unprecedented detail. Assignments based on molecular mass measurements have provided reasonable explanations for about 91–99% of the m/z 1000–2000 ESI ion current from the two proteins. The purified proteins consist of 18–20 different isoforms with predominant presence of the 5CHO glycoform and uneven representation of the 6-, 4-, 3-, 2- and 1CHO glycoforms, presumably reflecting varying susceptibility and/or resistance to the glycosidases to which the protein is normally exposed in the lysosome. Heterogeneity in the length of the amino acid chain is minimal with the 1–79 isoform accounting for more than 95% of the protein from both sources, and the 1–80 isoform being the only other detected. Again this presumably reflects the minimal molecular size that remains following lysosomal proteolytic exposure. It is possible that some of the isoforms represent covalent modifications formed during purification. The most likely of

these would be the oxidized molecules which were not unexpectedly in higher abundance in the HUA reflecting increased opportunity for oxidation before sample collection. The purification achieved by a single step of extended C_8 RP-HPLC following enzymatic deglycosylation yielded preparations that were free of the majority of the minor isoforms and provided samples that should be better suited for investigations such as by x-ray crystallography and NMR, which demand samples of greater purity.

The prosaposin gene contains a nine base pair exon within the CSAct region which is variably expressed in the isolated cDNAs.⁴⁴ However, with limits of detection conservatively estimated at <1% of the total ion current, we have not detected components in either HUA or PKA that would correspond to a species containing the three additional encoded amino acids (QDQ) of exon 8. Any proteins derived from exon 8-containing mRNAs are

apparently either unstable in the lysosomal milieu or are separated away in the course of purification.

The pattern of glycosylation found in HUA can be compared with that reported for human liver proteins by Yamashita *et al.*⁴⁵ Their material from normal liver contains a similar mixture of glycoforms. The 5CHO glycoform (Man₂GluNAc₂Fuc) was the most abundant component, accounting for 35–40% of the preparation. A 4CHO glycoform (Man₂GluNAc₂) was the next most abundant, with 1- (GluNAc), 2- (GluNAc₂), 4- (ManGluNAc₂Fuc) and 6CHO (Man₃GluNAc₂Fuc) glycoforms each accounting for about 10% of the sample. Two other 5- and 3CHO glycoforms (Man₃GluNAc₂, and ManGluNAc₂, respectively) accounted for the remaining 5% of the sample. None of the more complex oligosaccharide-containing materials found in liver from a patient with generalized gangliosidosis⁴⁵ was detected in the HUA reported here. It remains to be determined if the urine protein from patients with elevated CSAct accumulation is also more highly glycosylated.

The CSAct proteins demonstrated remarkable behavior during RP-HPLC. Isoforms containing the addition of a single molecule of oxygen could be cleanly separated from the unoxidized forms with baseline resolution, yet in the native proteins an additional C-terminal amino acid had a relatively minor effect on chromatographic behavior. The extension of retention time and peak sharpening following disulfide reduction is probably the result of exposure of additional surfaces in the reduced protein for interaction with the column. The interior of the CSAct molecule is thought to be more hydrophobic than the exterior surface,⁴⁶ and disulfide reduction would relax the structure, thus permitting interaction of these hydrophobic surfaces with the column matrix. This improved resolution with the disulfide reduced protein could be used advantageously to achieve even further protein purification should that be necessary.

Some aspects of the behavior of the protein are difficult to reconcile completely with our extant body of knowledge. For example, during ESI in 0.1% TFA native PKA emerges as predominantly the pentuply protonated molecule. However, slight elevation of the pH of the solvent by use of 0.1% formic acid results in the emergence of a predominantly higher charge state. In disulfide-reduced protein these two acids produced essentially identical spectra with predominance of the higher charge state. Generally an unfolded protein shows higher charge states than the same protein in the native state, although the physical basis for this relationship is still not completely understood.⁴⁷ PKA has eight residues that are potentially protonatable (Arg (2), Lys (3), His (2) and amino terminal). The maximum charge state of the protein is only seen as a minor component under the most favorable conditions. The observation that the charge state increases on going from TFA to formic or acetic acid appears counterintuitive and presumably reflects an obscure aspect of the tertiary structure of the protein in the gas phase. Alternatively, it may reflect differences between the ion pairing of the protein with TFA and with the other acids used (acetic and formic). The significance of this observation for the structure of the protein in the aqueous physiological environment remains to be appreciated. With formic and acetic acid, but not TFA, ESI ion current strength was favored

by the addition of acetonitrile, although there was no effect on charge state distribution. Organic co-solvents are traditionally thought of as assisting the ESI process by providing stable electrospray conditions, although the requirement for the organic co-solvent in this regard may be less critical for the IonSpray source used here. Previous work with hydrogen–deuterium exchange has revealed the stabilizing effect of acetonitrile on CSAct structure, presumably through occupancy of the hydrophobic core of the molecule by the organic modifier.⁴⁸ Apparently acetonitrile has no effect on the number of basic residues available for protonation, but it does influence the number of ionized molecules which are detected in the mass spectrometer.

The fragmentation of PKA protein by low-energy collisional activation required extreme conditions with high collision gas pressure and orifice and R₂ offset voltages, before any significant ion current could be observed in the *m/z* 50–2400 range. Even then the results with native and disulfide-reduced protein revealed a limited but similar repertoire of product ions which, with one exception, appear to be exclusively derived from fragmentation of the sugar moiety attached to Asn₂₁. This is attributable to the fact that the sugar residue is exposed on the outside surface of the molecule^{46,48,49} and is the only part of this otherwise tight compact molecule that can be broken off during the MS/MS experiment. The single exception is the fragment ion at *m/z* 1410 from disulfide-reduced protein. This fragment ion was formed in equal abundance from each of the glycoforms (1-, 2- and 5CHO). A listing of all possible fragment ions from this protein revealed a reasonable match with singly charged b₁₃ and y₁₃ ions. Inspection of the currently favored model for the protein⁴⁹ reveals that cleavage at the Gln₆₆–Pro₆₇ amide bond that would release the y₁₃⁺ ion. This is a possible site for fragmentation because it is located in a loop segment of the multi-helical barrel structure, joining the third and fourth helical segments. This fragment is not evident in the tandem mass spectra of the native protein, presumably because the internal disulfide bonds keep the structure intact. Confirmation of the assignment of y₁₃⁺ by using greater mass resolution for unambiguous charge state assignment and/or more accurate *m/z* assignment would provide support for the current structural model.

The attempts to demonstrate ions for physiologically meaningful non-covalent associations between CSAct molecules themselves and between CS and CSAct by mass spectrometry are to be contrasted with a growing volume of literature from other proteins and ligands on this subject^{50,51} (see Ref. 52 for a recent review). The dimeric nature of CSAct at pH 4–7 in aqueous buffers has been repeatedly demonstrated through the use of size-exclusion chromatography using OD₂₈₀ absorption for detection²⁴ (see Ref. 8 for a summary) and more recently through the use of light scattering detection (A. J. Waring *et al.*, unpublished observations). Furthermore, it is generally accepted that two molecules of protein bind a single molecule of CS. This stoichiometry has been demonstrated independently by several different laboratories (summarized in Ref. 8). However, repeated attempts to identify mass spectrometric conditions which favored gas-phase retention of the dimeric nature of the protein and the 2:1 binding stoichiometry between protein and lipid were only partially successful. These

results were obtained despite the use of conditions which favored heme binding to myoglobin (as a test case), CSAct dimerization and CS-CSAct binding. It is not clear that the low-abundance complexes observed at low buffer concentrations represent anything more than the non-specific interactions frequently observed in the electrospray process. However, with nanospray on the ESI/TOF instrument the apparent large relative abundance of the expected dimer and (dimer + 1 lipid) complexes at 100 mM buffer concentration supports the idea that these complexes result from specific interactions. Such observations of complexes at high salt concentrations with nanospray when nothing is observed under low salt conditions have been made for a number of complexes at Manitoba, and have been reported also for the HU protein.⁵³ Nevertheless, under the most favorable conditions the ions for the dimer and the [dimer + 1 lipid] were always accompanied by ions of similar or greater abundance for the monomeric protein.

Two explanations can be offered for these results. One possibility is simply that conditions were not used

which favored complete retention of non-covalent associations in the gas phase with this protein. Our preferred explanation is that non-covalent associations with this protein (both dimerization and ligand binding) are largely hydrophobic in nature. In the gas phase the complete absence of water molecules attached to the protein results in loss of the hydrophobic forces and dissociation to monomeric protein free of ligand. This explanation will be tested as results are reported for other protein-ligand complexes which rely heavily on hydrophobic forces.

Acknowledgements

This work was supported by grants from the NIH (NS31271, P.I. ALF.) and the W. M. Keck Foundation. Ken Conklin and UCLA undergraduate Student Research Project participants Babak Shabatin, Kelly Roy and Kevin Chou helped with the preparation of the DTT-guanidine-treated protein. The work at Manitoba was supported by grants from NSERC (Canada), and benefited greatly from preliminary measurements by Igor Chernushevich.

REFERENCES

1. Sacchettini JC, Gordon JI, Banaszak LJ. *J. Biol. Chem.* 1988; **263**: 5815.
2. Segrest JP, Jackson RL, Morrisett JD, Gotto Jr AM. *FEBS Lett.* 1974; **38**: 247.
3. Munford RS, Sheppard PO, O'Hara PJ. *J. Lipid Res.* 1995; **36**: 1653.
4. Ponting CP, Russell RB. *Trends Biochem. Sci.* 1995; **20**: 179.
5. Liepinsh E, Andersson M, Ruysschaert J-M, Otting G. *Nature Struct. Biol.* 1997; **4**: 793.
6. Mehl E, Jatzkewitz H. *Hoppe-Seyler's Z. Physiol. Chem.* 1963; **331**: 292.
7. Mehl E, Jatzkewitz H. *Hoppe-Seyler's Z. Physiol. Chem.* 1964; **339**: 260.
8. Fluharty AL. *Trends Glycosci. Glycotechnol.* 1995; **7**: 167.
9. O'Brien JS, Kishimoto Y. *FASEB J.* 1991; **5**: 301.
10. Sandhoff K, Harzer K, Fürst W. In *The Metabolic and Molecular Bases of Inherited Disease* (7th edn). Scriver CR, Beaudet AL, Sly WS, Valle D (eds). McGraw-Hill: New York, 1995; 2427.
11. Fürst W, Sandhoff K. *Biochim. Biophys. Acta* 1992; **1126**: 1.
12. Conzelmann E, Sandhoff K. *Methods Enzymol.* 1987; **138**: 792.
13. Inui K, Wenger DA. *Arch. Biochem. Biophys.* 1984; **233**: 556.
14. Li SC, Sonnino S, Tettamanti G, Li Y-T. *J. Biol. Chem.* 1988; **263**: 6588.
15. Stevens RL, Fluharty AL, Kihara H, Kaback MM, Shapiro LJ, Marsh B, Sandhoff K, Fischer G. *Am. J. Hum. Genet.* 1981; **33**: 900.
16. Gieselmann V, Zlotogora J, Harris A, Wenger DA, Morris CP. *Hum. Mutat.* 1994; **4**: 233.
17. Kolodny EH, Fluharty AL. In *The Metabolic Molecular Basis of Inherited Disease* (7th edn). Scriver CR, Beaudet AL, Sly WS, Valle D (eds). McGraw-Hill: New York, 1995; 2693.
18. O'Brien JS, Kretz KA, Dewji N, Wenger DA, Esch F, Fluharty AL. *Science* 1988; **241**: 1098.
19. Nakano T, Sandhoff K, Stümper J, Christomanou H, Suzuki K. *J. Biochem.* 1989; **105**: 152.
20. Rorman EG, Grabowski GA. *Genomics* 1989; **5**: 486.
21. Dewji NN, Wenger DA, O'Brien JS. *Proc. Natl. Acad. Sci. USA* 1987; **84**: 8652.
22. Fisher G, Jatzkewitz H. *Biochim. Biophys. Acta* 1977; **481**: 561.
23. Vogel A, Schwarzmann G, Sandhoff K. *Eur. J. Biochem.* 1991; **200**: 591.
24. Fluharty AL, Katona Z, Meek WE, Frei K, Fowler AV. *Biochem Med. Metab. Biol.* 1992; **47**: 66.
25. Fluharty AL, Lombardo C, Louis A, Stevens RL, Whitelegge J, Waring AJ, Fluharty C, Faull KF. *Mol. Genet. Metab.*, in press.
26. Fluharty AL, Davis ML, Kihara H, Kritchevsky G. *Lipids*, 1974; **9**: 865.
27. Whitelegge JP, Faull KF, Penn B, To T, Waring A, Fluharty C, Fluharty AL. In *New Methods for the Study of Biomolecular Complexes*. Ens W, Chernushevich I, Standing K (eds). NATO ASI Science Series, Kluwer Academic: Dordrecht, 1998; 67.
28. Fluharty AL, Meek WE, Katona Z, Tsay KK. *Biochem. Med. Metab. Biol.* 1992; **47**: 86.
29. Glasgow BJ, Abduragimov AR, Yusifov TN, Gasymov OK, Horwitz J, Hubbell WL, Faull KF. *Biochemistry*, 1998; **37**: 2215.
30. Lee TD, Vemuri S. *Biomed. Environ. Mass Spectrom.* 1990; **19**: 639.
31. Roepstorff P, Fohlman J. *Biomed. Mass Spectrom.* 1984; **11**: 601.
32. Biemann K. *Biomed. Environ. Mass Spectrom.* 1988; **16**: 99.
33. Krutchinsky AN, Chernushevich IV, Spicer VL, Ens W, Standing KG. *J. Am. Soc. Mass Spectrom.* 1998; **9**: 569.
34. Wilm MS, Mann M. *Int. J. Mass Spectrom. Ion Processes* 1994; **136**: 167.
35. Stevens RL, Faull KF, Conklin KA, Green BN, Fluharty AL. *Biochemistry* 1993; **32**: 4051.
36. Collard MW, Sylvester SR, Tsuruta JT, Griswold MD. *Biochemistry* 1988; **27**: 4557.
37. Tsuda M, Sakiyama T, Endo H, Kitagawa T. *Biochem. Biophys. Res. Commun.* 1992; **184**: 1266.
38. Azuma N, Seo H-C, Lie Ø, Fu Q, Gould RM, Hiraiwa M, Burt DW, Paton IR, Morrice DR, O'Brien JS, Kishimoto Y. *Biochem J.* 1998; **330**: 321.
39. Fürst W, Schubert J, Machleidt W, Meyer HE, Sandhoff K. *Eur. J. Biochem.* 1990; **192**: 709.
40. Ludwig ML, Hunter MJ. *Methods Enzymol.* 1967; **11**: 595.
41. Konigsberg WH, Steinman HM. In *The Proteins* (3rd edn), vol. III. Neurath H, Hill RL (eds). Academic Press: New York: 1977; 1.
42. Hsu F-F, Bohrer A, Turk J. *Biochim Biophys. Acta* 1998; **1392**: 202.
43. Marbois BM, Faull KF, Fluharty AL, Raval-Fernandes S, Rome LH. Submitted.
44. Holtschmidt H, Sandhoff K, Fürst W, Kwon HY, Schnabel D, Suzuki K. *FEBS Lett.* 1991; **280**: 267.
45. Yamashita K, Inui K, Totani K, Kochibe N, Furukawa M, Okada S. *Biochemistry* 1990; **29**: 3030.

46. Waring AJ, Chen Y, Faull KF, Stevens R, Sherman MA, Fluharty AL. *Mol. Genet. Metab.* 1998; **63**: 14.
47. Konermann L, Douglas DJ. *Biochemistry* 1997; **36**: 12296, and references cited therein.
48. Faull KF, Higginson J, Waring AJ, To T, Whitelegge JP, Stevens RL, Fluharty C, Fluharty AL. Submitted.
49. Whitelegge JP, Penn B, To T, Waring AJ, Sherman M, Stevens RL, Fluharty C, Fluharty AJ, Faull KF. Submitted.
50. Ganem B, Li Y-T, Henion JD. *J. Am. Chem. Soc.* 1991; **113**: 6294.
51. Ganem B, Li Y-T, Henion JD. *J. Am. Chem. Soc.* 1991; **113**: 7818.
52. Loo JA. *Mass Spectrom. Rev.* 1997; **16**: 1.
53. Vis H, Heinemann U, Dobson CM, Robinson CV. *J. Am. Chem. Soc.* 1998; **120**: 6427.